

Structural optimization of monosymmetrical non-circular hole on engine turbine disk based on EAGA with modified immigrant strategy

Qiu Ren Chen¹, Hai Ding Guo , Hai Tao Cui

¹ Nanjing University of Aeronautics and Astronautics, Nanjing, Jiangsu, China, nuaacqr@126.com

1. Abstract

The bolt-holes, pin-holes and vent holes on aero-engine disc are in many cases the most critical regions, and there exists high level stress concentration around these areas. This paper proposed a parameterized model of non-circular-hole, the profile of which could be optimized for different structural load conditions, to improve fatigue performance of the holes and that of the aero engine disk as well. An optimum design based on thermal-structural finite element analysis on a high-pressure turbine disk is conducted, and stress concentration around the optimized non-circular-holes could be dramatically reduced. In the paper, an elite-preservation adaptive genetic algorithm with modified immigrant strategy is used in the algorithm. After optimizing, the stress concentration is evidently decreased and the maximum first principal stress is reduced for 17.37%. The analysis of design variables' sensitivity shows that the dimensions of transition arcs which connect main arcs are of significant effect on the stress concentration on the holes' edge.

2. Keywords: structural optimization; non-circular-hole; elite-preservation adaptive genetic algorithm; sensitivity analysis.

Nomenclature			
a	Maximum half horizontal height	C_{sim}	Similarity ratio of the current population
b	Maximum half vertical width	C_{cr}	Critical value of similarity
R_1	Top arc radius	ΔI_i	Chaotic disturbance
R_2	Bottom arc radius	N_g	Number of generation
R_3	Lateral main arc radius	K_1	Maximum first principal stress drop ratio
R_4	Upper transition arc radius	σ_{1max}	Maximum first principal stress
R_5	Bottom transition arc radius		

3. Introduction

Assemble holes, pin holes and vent holes of turbine disc or compressor disc are critical regions for which life certification is necessary. The loads associated with these regions are the centrifugal forces on the disc and associated blades, thermal loads, and there exists high level stress concentration around holes' areas[1-2].

To resolve hole stress concentration problems, technicians adopted some implementations such as chamfering and polishing, and some surface treatment processes are also applied. However, even with all those technical processes, we can not effectively decrease the stress concentration around those areas, the thermo-mechanical integrity of turbine discs is crucial to the operational safety and service life of gas turbine engines [4-8].

One effective approach to smooth the stress concentration is to change the profile of the hole. Non-circular hole can be the candidate of it. This shape-design methodology is firstly applied in the tunnel wall design for the purpose of decreasing the stress concentration. However, only fragmentary information towards the non-circular holes design of aero engine disc has been reported till now [9].

Generally, the profile of a non-circular hole must be smooth and continuous to reduce stress concentration. When bolt holes are considered, the fit tolerance of hole and bolt should not be altered. Additionally, to ensure a moderate machining cost, the minimum radius of the profile should refer to the geometry of cutting tools.

In the paper, in consideration of the requirements above, a mathematical model of non-circular hole is built. We take primal hole as a base circle and the profile of the hole consists of eight smoothly connected arcs. A turbine disc with such a non-circular bolt hole on its collar is modeled and analyzed. A finite element model is built for it and the dimensions of the hole are optimized, in which a modified Elite Preservation-Adaptive Genetic Algorithm (EP-AGA) is proposed and an immigrant strategy is added to speed up convergence.

4. Geometric modeling of non-circular hole

4.1 Basic agreement

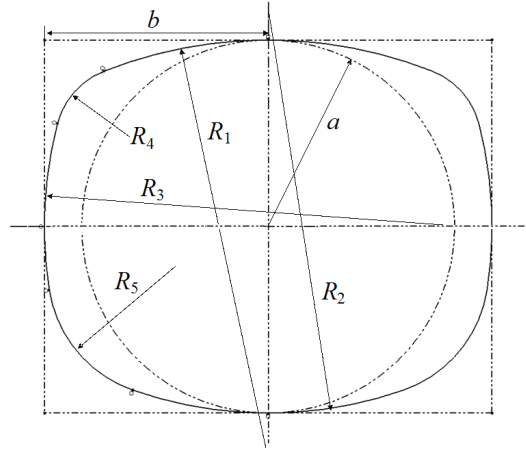


Figure 1: Geometry model of non-circular hole

The non-circular hole is symmetrical to Y axis. Its profile consists of a top main arc (radius= R_1), a bottom main arc (radius= R_2), two lateral main arcs on both sides (radius= R_3), two upper transition arcs (radius= R_4) and two bottom transition arcs (radius= R_5). R_1 、 R_2 、 R_3 、 R_4 and R_5 are chosen as independent design variables for the following optimization.

Since the non-circular hole is symmetrical to Y axe, a quarter of the hole in second quadrant is studied.

4.2 Constraint functions

According to Figure 1, R_1 、 R_2 should be greater than a as in Eq. (1), which guarantees the smooth connection between transit segment (R_3), main arcs (R_1 and R_2).

$$\begin{cases} R_1 > a \\ R_2 > a \end{cases} \quad (1)$$

As transition segment between R_1 and R_2 , R_3 is in the second quadrant and can be expressed by Eq. (2)

$$R_3 < a \quad (2)$$

Based on the geometrical relations of arcs connection, the center coordinates of arc R_3 are derived and given in Eq.

(3), which ensures the smooth connection among R_3 - R_1 and R_3 - R_2

$$\begin{cases} X_3 = \frac{-en - 2nm^2 - \sqrt{-e^2 m^2 + 4em^2 n^2 + 4j^2 m^2 n^2 - 4m^2 n^4 + 4j^2 m^4}}{2(m^2 + n^2)} \\ Y_3 = \frac{em - 2mn^2 + \sqrt{-e^2 n^2 - 4em^2 n^2 + 4i^2 m^2 n^2 - 4m^4 n^2 + 4i^2 n^4}}{2(m^2 + n^2)} \end{cases} \quad (3)$$

where $m = R_1 - a$, $n = a - R_2$, $i = R_1 - R_3$, $j = R_2 - R_3$, $e = i^2 - j^2 + n^2 - m^2$. In the mean time, coordinates of the tangent point P between R_3 and R_1 can be given by Eq. (4)

$$\begin{cases} x_p = -\frac{R_1}{g} \\ y_p = \frac{-mR_1 - R_1 y_3 - g m x_3}{g x_3} \end{cases} \quad (4)$$

where g is given by Eq. (5)

$$g = \sqrt{1 + \left(\frac{y_3 + m}{x_3}\right)^2} \quad (5)$$

the coordinates of tangent point Q between R_2 and R_3 can be calculated in Eq. (6)

$$\begin{cases} x_q = \frac{-n - f^2 n - \sqrt{R_2^2 + f^2 R_2^2}}{1 + f^2} \\ y_q = -\frac{f \sqrt{(1 + f^2) R_2^2}}{1 + f^2} \end{cases} \quad (6)$$

Where f is given by Eq. (6)

$$f = \frac{y_3}{x_3 + n} \quad (7)$$

For the second quadrant arcs, the coordinates of the tangent points must also meet the need of the constraints given by Eq. (8)

$$\begin{cases} -a < x_p < 0, a > y_p > 0 \\ -a < x_q < 0, a > y_q > 0 \end{cases} \quad (8)$$

When the center coordinates of R_3 are given by Eq. (3), R_1 and R_2 are given by Eq. (1), transition arcs will be tangent to the main arcs respectively. The coordinates of tangents points meet the need of Eq. (4) and (5) too. Other quadrant arcs connect in a similar geometric relationship. In the mean time, the fit tolerance of hole and bolt will be the same as the primal bolt hole.

5. Optimization example of bolt holes on the turbine collar

5.1 Thermal-structural analysis

A turbine disc of an aero-engine is selected as an example. The turbine disc is considered a symmetrical one, with two collars on each side. The bolt holes are on the collars of the discussed. A segment of turbine disc model is shown in Figure 2.

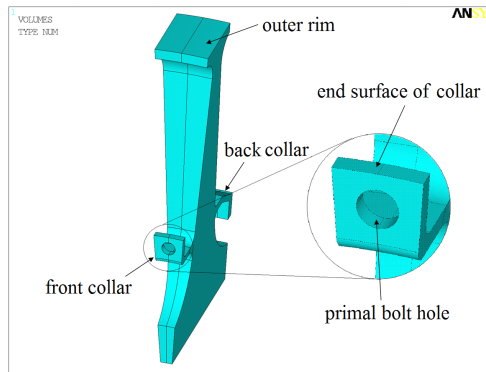


Figure 2: Simplified model of the turbine disk fan-shaped segment

In the analysis, both mechanical load and heat load are considered, based on the hypothesis of steady-state heat transferring process and the first thermal boundary conditions are considered. The structure platforms and blades are neglected and replaced by equivalent centrifugal load on the outer edge of the disc (shown in Figure 2). The compressive load on the wall of bolt hole is not considered. Element SOLID 87 is used in the thermal stress analysis, which is then transformed into element SOLID 187 in the structural analysis. The rotational speed is 12000 rpm. GH4169 is chosen as the material of the disk model and its properties in different temperatures are shown in Figure 3 as below.

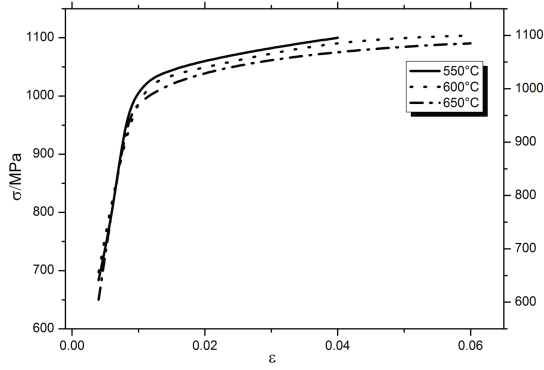


Figure 3: Material properties of GH4169 under 550°C、600°C and 650 °C

5.2 Elite-preservation adaptive genetic algorithm (GA) with modified immigrant strategy

The optimization algorithm is based on the elite-preservation adaptive genetic algorithm which guarantees the global optimal solution.

In practice, GA is associated with defects like premature or poor convergence. In the paper, a modified immigrant strategy prior to crossover operation is proposed, which can enhance diversity of the population and be used to get rid of premature.

Before implementing the immigrant strategy, a parameters C_{sim} is calculated to evaluate the similarity of current population and is given by

$$C_{sim} = \sum_{i=1}^{n=Ng} \sum_{j=i+1}^{n=Ng-i} \frac{1}{(x_i \oplus x_j)} \quad (9)$$

where Ng stands for the number of generation. It can be seen, the larger the C_{sim} , the more intensive the similarity among individuals of the population. When C_{sim} is over critical value C_{cr} which is defined as 0.08 in the article, a number of new immigrant individuals will be supplemented to improve the diversity of the population. The genes of immigrant individuals are formed based on the best individuals of the previous generation, and modified by a moderate chaotic disturbance ΔI_i . The value of immigrant individual- x_{im} is defined as Eq. (10)

$$x_{im} = x_{best} + \Delta I_i \quad (10)$$

Where x_{best} is one of the best sets and ΔI_i is defined in Eq. (11)

$$\Delta I_i = x_n \cdot (x_{best} - x_{worst}) \quad (11)$$

where x_n is a chaotic vector mapped from the current individual x_{im} . The insect amount model is selected to carry out the chaotic mapping. The insect amount model is a typical chaotic model, which is defined as follow

$$x_j = \mu * x_j * (1 - x_j) \quad \mu \in [0, 4] \quad (12)$$

where x_{j+1} , x_j are two vectors mapped from the best sets of current and previous generations to 0~1, which stand for the insects number of the current and previous generations. The n stands for the number of generation, which is 50. The μ stands for a constant (defined as 3.8) that controls the convergence property of the system. When μ is over 3.3, the system presents a highly non-linear property and becomes chaotic, which will maintain the diversity of the individuals in the generation.

5.3 Process integration

The maximum first principal stress on the surface (σ_{1max}) of the hole is chosen as criterion function. Eq. (13) gives the optimization model

$$\begin{cases} \min f(R_i) = \sigma_{1max}, & (i=1, 2, 3, 4, 5) \\ s.t. R_1 > a, R_2 > a, R_3 > a \\ a > R_4 > R_{min}, a > R_5 > R_{min} \end{cases} \quad (13)$$

where $R_1 \sim R_5$ are five design variables. R_{min} is the minimum processing radius of cutting-tools. According to the reference [11], let $R_{min}=2mm$. In order to evaluate optimization results, a descent ratio of maximum first principal stress (K_1) on inner surface is described by

$$K_1 = \frac{(\sigma_{1\max} - \sigma_{1\max 0})}{\sigma_{1\max 0}} \times 100\% \quad (14)$$

where $\sigma_{1\max 0}$ is the maximum first principal stress on the edge of circular hole, $\sigma_{1\max}$ is the one on the optimized non-circular hole. Figure 4 is the flowchart of the optimization process for non-circular hole.

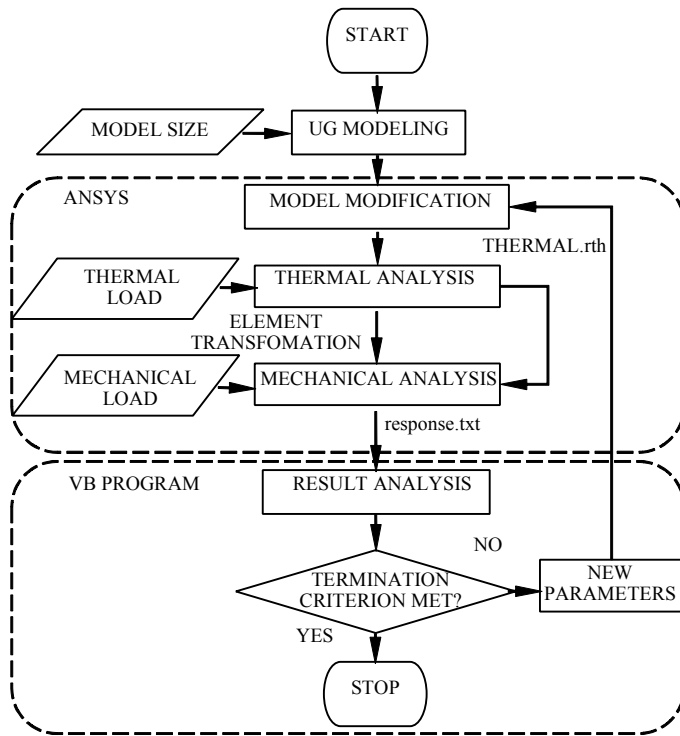


Figure 4: Integration of optimization process

6. Optimization results

The optimum design is carried out based on the proposed algorithm in section 3.2 and the results are tabulated in Table 2.

Table 2: Optimization results with objective function $\sigma_{1\max}$

Design parameters	R_1/mm	R_2/mm	R_3/mm	R_4/mm	R_5/mm	$\sigma_{1\max}/\text{MPa}$	$K_1/\%$
Primal circular hole	5.25	5.25	5.25	5.25	5.25	831.2	N/A
Initial non-circular hole	16.40	19.30	20.50	3.50	2.90	729.3	12.26
Optimum non-circular hole	19.30	20.40	22.30	2.50	2.20	686.8	17.37

The data in Table 2 indicates that compared with $\sigma_{1\max 0}$ on a circular hole, the lowest $\sigma_{1\max}$ in the first generation for non-circular hole is 12.26% lower than the $\sigma_{1\max 0}$ on circular hole. After optimization, the $\sigma_{1\max}$ on non-circular hole dropped another 5.4%. In comparison with circular hole, the optimum radius of main arcs, especially the lateral main arc R_2 , are much larger, and this makes the profile of the non-circular hole flatter. The optimization history of objective function is shown in Figure 5.

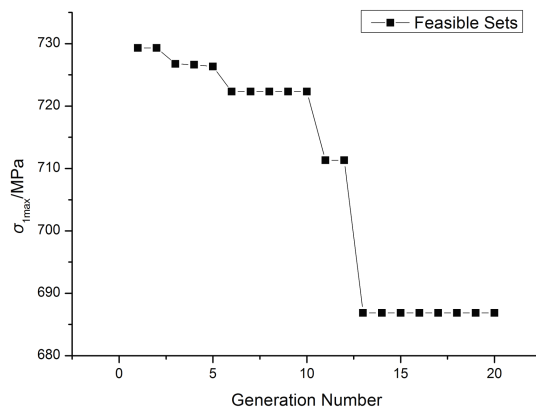


Figure 5: optimization history of objective function σ_{1max}

As shown in Figure 5, σ_{1max} on the edge of non-circular hole achieves a significant decrease after optimizing. Within the scope, a larger R_1 will be beneficial for decrease of the stress and strain. The first principal stress nephogram of collars (cut from the disk) with primal circular hole and optimum non-circular hole are shown in Figure 6 and Figure 7 respectively.

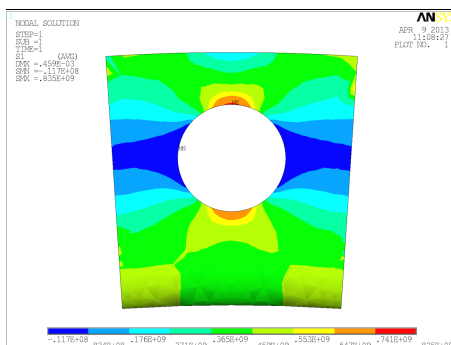


Figure 6: First principal stress nephogram of the collar with a primal circular hole

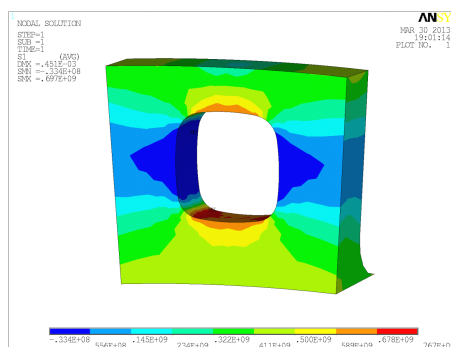


Figure 7: First principal stress nephogram of the collar with an optimum non-circular hole

As for the optimized non-circular hole in Figure 7, six o'clock area of the hole is the most dangerous one, yet the average stress of the dangerous area remarkably fell compared with original circular hole. The high stress areas are located at the top and bottom main arcs. After optimization, approximate 13.2% first principal stress on the edge of the hole is reduced in comparison with the circular hole. Meanwhile, stress distribution on the edge of the hole is more balanced and beneficial. The von mises stress of stress concentration region spread from 500MPa to 700MPa. The optimum profile of non-circular hole also suggests that flatness for top and lateral main arcs is beneficial for

relieving stress concentration on the hole edge, and decreasing the first principal stress and von mises stress as well.

7. Sensitivity analysis

In order to investigate the impacts of design variables towards objective function σ_{1max} , sensitivity analysis is conducted after optimization. The PDS module of ANSYS is used, integrating Monte Carlo probabilistic design method and FEM, to calculate the probabilistic sensitivity of the design variables towards σ_{1max} on the edge of non-circular hole. The level of sensitivity is characterized by spearman correlation coefficient. The results of sensitivity analysis are shown in table 3, and the proportion of each correlation coefficient is shown in Figure 9.

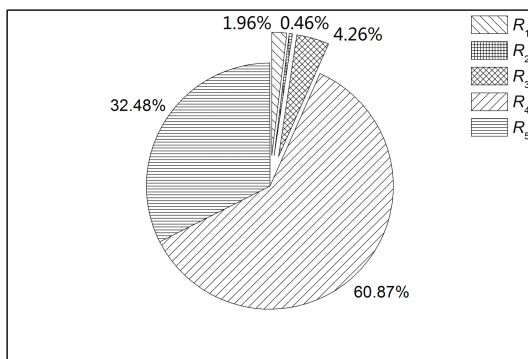


Figure 9: Sensitivity proportion of design variables towards σ_{1max}

Figure 9 shows that the correlation coefficient absolute value of R_4 and R_5 towards σ_{1max} is larger than other design variables, which means the variation of R_4 and R_5 contributes more to the variation of σ_{1max} .

8. Conclusion

Aiming at the stress concentration problem on aero engine turbine disks, this paper proposed a parameterized model of non-circular-hole, of which the profile is made up by eight smoothly connected arcs and could be converted for different structural load conditions, to improve fatigue performance of pilot holes and that of the aero engine disk as well.

The optimal computation is based on the proposed adaptive genetic algorithm with chaotic immigrant strategy and is realized through Visual Basic programming. The conclusions can be drawn as follow: ① A well designed non-circular hole could evidently reduce stress concentration on hole edge, thereby boosting the structural service life of the disk. ② Through optimum design, σ_{1max} on the non-circular hole edge could drop for over 17.36% compared with circular hole. ③ Sensitivity analysis on design variables suggests that impacts of transition arcs R_4 and R_5 towards σ_{1max} are more significant than R_1 、 R_2 and R_3 .

9. Acknowledgements

I would like to take this chance to express my sincere gratitude to my supervisor, Prof. Guo, for his kindly assistance and valuable suggestions during the process of my paper writing. His willingness to give his time so generously has been very much appreciated. My gratitude also extends to Prof. Cui, for his kind encouragement and patient instructions. Last but not the least, I would like to offer my particular thanks to the research fellows in my lab, for their encouragement and support for the completion of this paper.

10. References

[1] W Li, L W Dong, et al. Structure analysis and life evaluation of the pin holes in a turbine disk of a type of aero-engine. *Journal of Aerospace Power*, 24(8):1699-1706, 2009.

10th World Congress on Structural and Multidisciplinary Optimization

May 19 -24, 2013, Orlando, Florida, USA

- [2] S Lu, Q Q Huang, et al. New method for damage tolerance analysis of turbine disk and its application. *Journal of Aerospace Power*, 17(1):87-92, 2002.
- [3] Y J Shi, M Wang. Analysis on shear behavior of high-strength bolts connection. *International Journal of Steel Structures*, 11(2):203-213, 2011.
- [4] N L Pedersen. Optimization of bolt thread stress concentrations. *Archive of Applied Mechanics* (2):1-14, 2012.
- [5] Y Gao, G C Bai, et al. Reliability analysis of multi-axial low cycle fatigue life for turbine disk. *Acta Aeronautica et Astronautica Sinica*, 30(9):1678-1782, 2009.
- [6] Z Tan, D X Liu, et al. Fatigue behavior of TC16 titanium alloy bolts and 30CrMnSiA steel joint holes. *Mechanical Science and Technology*, 25(7):767-770, 2006.
- [7] Q R Liu, Y P Liu. Crack failure analysis of the 4th engine compressor disk. *Aero Engine*, 2:38-41, 1999.
- [8] A Z Lu, Q W Wang. New Method of determination for the mapping function of tunnel with arbitrary boundary using optimization techniques. *Chinese Journal of Rock Mechanics and Engineering*, 14(3): 269-274, 1995.
- [9] G Chen. Structural designing and developing characteristics of CFM56 series engines. *Beijing University of Aeronautics and Astronautics Press*, 2006.
- [10] H Y Xu. Study on connection of friction-typed multiple-row high-strength bolt. *Journal of Railway Engineering Society*, 11(158):67-71, 2011.
- [11] X Wei. Study on machining process of shaped hole in Ni-base super-heat-resistant alloy work pieces. *Tool Engineering*, 36(6):19-23, 2002.